Network Dynamics - Homework 2

December 11, 2022

Abstract

In this report, we present our solution to Homework 2. This report is the result of the active collaboration between: Lorenzo Bergadano (s304415), Francesco Capuano (s295366), Matteo Matteotti (s294552), Enrico Porcelli (s296649), and Paolo Rizzo (s301961). For the sake of full reproducibility, we published our code on GitHub at: https://github.com/fracapuano/NetworkDynamics.

1 Exercise 1

Consider the graph presented in Figure 1.

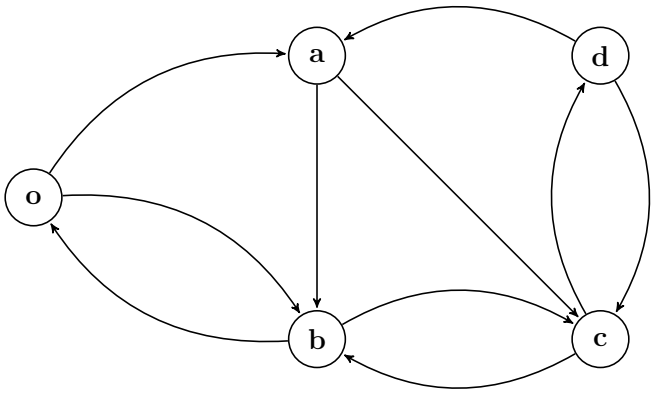

Figure 1: Exercise 1 network

With the following rate transition matrix:

$$\Lambda = \begin{pmatrix} 0 & 2/5 & 1/5 & 0 & 0 \\ 0 & 0 & 3/4 & 1/4 & 0 \\ 1/2 & 0 & 0 & 1/2 & 0 \\ 0 & 0 & 1/3 & 0 & 2/3 \\ 0 & 1/3 & 0 & 1/3 & 0 \end{pmatrix} \tag{1}$$

Indexed, in the same order of their appearance, by the elements of the set $\mathcal{V} = \{o, a, b, c, d\}$. We answered the following questions related to *continuous-time* walks in the considered setting:

Question (a) What is, according to numerical simulations of the system, the average time it takes a particle that starts in node a to leave the node and then return to it?

Question (b) How does the result in *Question (a)* compare to the theoretical return-time $\mathbb{E}_a(T_a^+)$

Question (c) What is, according to numerical simulations of the system, the average time it takes to move from node o to node d?

Question (d) How does the result in *Question (c)* compare to the theoretical hitting-time $\mathbb{E}_o(T_d)$?

Question (e) Interpret the matrix Λ as the weight matrix of a graph $\mathcal{G} = (\mathcal{V}, \mathcal{E}, \Lambda)$, and simulate the French-DeGroot dynamics on $\mathcal{G}$ with an arbitrary initial condition $x(0)$. Do the dynamics converge to a consensus state for every initial condition $x(0)$?

Question (f) Assume that the initial state of the dynamics for each node $i \in \mathcal{V}$ is given by $x_i(0) = \xi_i$, where $\{\xi_i\}_{i\in\mathcal{V}}$ are *i.i.d* random variables with variance σ^2. Compute the variance of the consensus value, and compare the results with numerical simulations.

Question (g) Remove the edges (d, a) and (d, c). Describe and motivate the asymptotic behavior of the dynamics. If the dynamics converge to a consensus state, how is the consensus value related to the initial condition $x(0)$? Assume that the initial state of the dynamics for each node $i \in \mathcal{V}$ is given by $x_i(0) = \xi_i$, where $\{\xi_i\}_{i\in\mathcal{V}}$ are *i.i.d* random variables with variance σ^2. Compute the variance of the consensus value.

Question (h) Consider the graph $\mathcal{G}(\mathcal{V}, \mathcal{E}, \Lambda)$, and remove the edges (c, b) and (d, a). Analyze the French-DeGroot dynamics on the new graph. In particular, describe and motivate the asymptotic behavior of the dynamics in terms of the initial condition $x(0)$.

1.1 Question (a)

Let us first define the vector ω of the degrees of each node in $\mathcal{G}$ as:

$$\omega = \Lambda \mathbb{1} \tag{2}$$

Where $\mathbb{1}$ is the usual vector of all ones.

First of, it is worth mentioning that, unlike their discrete-time counterpart, random walks considered to happen in *continuous time* (as the one simulated in this Exercise) not only evolve randomly for what concerns their trajectory (i.e., the actual nodes that they visit. This aspect is common to both continuous and discrete random walks), but also for the amount of time they spend in each node.

To decline the Markov property in this context, one can rely on a memory-less distribution for the time spent in each node, since, to respect the aforementioned Markov property, one has to guarantee that the process' evolution only depends on the current state and is independent on the whole past. Recalling that the exponential distribution is indeed memory-less, it comes naturally to assume that the time a walker spends in node i is a random variable distributed according to an exponential distribution of parameter ω_i.

Therefore, the actual evolution of the trajectory can be simulated considering a process in which the evolution is fully node-dependent, and that therefore can be summarized in the two following steps:

(1) Await $t_{next} \overset{\text{drawn}}{\sim} Exp(\omega_i)$ time units (t.u.) in node i

(2) Move to any neighbouring node j according to probability P_{ij}

Where P is a matrix whose entries are defined as:

$$P_{ij} = \begin{cases} \frac{\Lambda_{ij}}{\tilde{\omega}_i}, & \text{if } \omega_i \neq 0 \\ 1, & \text{otherwise} \end{cases} \tag{3}$$

It is clear that once in node j, the just presented two-step process shall simply be repeated as is.

Using this approach, we simulated a random walk considering as a stopping condition for the trajectory evolution that the starting and the end node were both a, as well as requiring that the very same process would, at least, exit node a moving somewhere else to, only later on, return to a. Let us indicate the i-th measurement of the duration of the said process with $(T_a^+)_i$.

Our (empirical) estimate $(\tilde{\mathbb{E}}_a(T_a^+))$ of the average over $N = 5000$ simulations of the just mentioned process equates to:

$$\tilde{\mathbb{E}}_a(T_a^+) = \frac{1}{N}\sum_{i=1}^{N}(T_a^+)_i \simeq 6.7254 \text{ t.u.} \tag{4}$$

For full reproducibility of our experiments, we report we observed this value to fluctuate between different runs, although only marginally (typically, $\pm$ 0.002).

1.2 Question (b)

Let us first indicate with $\bar{\pi}$ the invariant probability of $\mathcal{G}$, i.e. that state that, once encountered, does not trigger any change in the dynamic.

Since a continuous-time Markov process can be described by the relationship:

$$\dot{x}(t) = -L^\intercal x(t) \tag{5}$$

In Newton's derivatives notation.

It is clear that invariant states for $\mathcal{G}$ (i.e., probability vectors) are all those vectors $\bar{\pi} \in [0,1]^{\mathcal{V}}$ such that:

$$\dot{\bar{\pi}}(t) = -L^\intercal \bar{\pi}(t) = 0 \tag{6}$$

Equivalently, invariant probabilities are the orthonormal basis of $L^\intercal$'s kernel. Moreover, this invariant probabilities vector is unique.

For the graph presented in Figure 1 this vector is:

$$\bar{\pi} = \begin{pmatrix} 0.1851 \\ 0.1481 \\ 0.2222 \\ 0.2222 \\ 0.2222 \end{pmatrix} \tag{7}$$

To obtain the theoretical return time (i.e. $\mathbb{E}_a(T_a^+)$), is sufficient to recall that:

$$\mathbb{E}(T^+) = (\mathbb{1}^\intercal \; diag(\omega)^{-1} \; diag(\bar{\pi})^{-1})^\intercal \tag{8}$$

Which implies:

$$\mathbb{E}_a(T_a^+) = \frac{1}{\bar{\pi}_a \omega_a} = 6.7500 \text{ (t.u.)} \simeq \tilde{\mathbb{E}}_a(T_a^+) \tag{9}$$

1.3 Question (c)

This question was answered partially reproducing the solution we developed for Question (a).

In particular, we simulated the chain from node o and iterated until the chain reached node d. We repeated this process N times and obtaining each time a measurement of the duration of said process equal to T^i_{o-d}. Later on, we obtained an empirical estimate of the Average $o-d$ Hitting Time, $\tilde{\mathbb{E}}_o(T_d)$.

In particular,

$$\tilde{\mathbb{E}}_o(T_d) = \frac{1}{N}\sum_{i=1}^{N} T^i_{o-d} \simeq 8.8220 \text{ (t.u.)} \tag{10}$$

For full reproducibility of our experiments, we report we observed this value to fluctuate between different runs, although only marginally (typically, $\pm$ 0.004).

1.4 Question (d)

To obtain the Expected $o-d$ Hitting Time it is sufficient recalling that, if one indicates with $T^{\mathcal{S}}_o$ the Hitting Time from node o to a subset $\mathcal{S}$ globally reachable in $\mathcal{G}$, then $\mathbb{E}(T^{\mathcal{S}}_o)$ is the unique solution of the system:

$$\begin{cases} \mathbb{E}(T^s_o) = 0 \quad \forall s \in \mathcal{S} \\ \mathbb{E}(T^s_o) = \frac{1}{\omega_s} + \sum_{j\in\mathcal{V}} P_{sj}\mathbb{E}(T^s_j) \quad \forall s \in \mathcal{V}\setminus\mathcal{S} \end{cases} \tag{11}$$

Which can clearly be represented in its matricial form denoting with $\overline{P}$ the matrix obtained removing the rows and columns associated with node d from P. Moreover, let us indicate with w the vector whose i-th is the inverse of the i-th entry of ω. Then 11 can be compactly rewritten as:

$$\mathbb{E}(T^{\mathcal{S}}_o) = w + \overline{P}\mathbb{E}(T^{\mathcal{S}}_o) \tag{12}$$

Which admits a unique solution when 1 is not in $\rho(\overline{P})$, which is always the case as long as (as per assumption of global reachability) there is at least one link from $\mathcal{V}\setminus\mathcal{S}$ to $\mathcal{S}$.

In particular, we obtained that:

$$\mathbb{E}(T^d_o) = 8.7857 \text{ (t.u.)} \simeq \tilde{\mathbb{E}}_o(T_d) \tag{13}$$

1.5 Question (e)

Let us briefly recall that an opinion dynamics model is a model in which states x represent agents' "opinions", which can easily encoded using either integers or real numbers depending on the context. Opinion dynamics models do capture the process with which agents update their opinion over time in light of other agents opinions, weighing the information sent by their neighbours with respect to the normalized weight matrix $P = D^{-1}W$. In particular, assuming that interactions take place at discrete instants of time, each of these interactions can be seen to contribute to the agents updating their opinion. This is reflected in the network state x evolving according to:

$$x(t+1) = Px(t), \quad t = 0, 1, 2, \ldots \tag{14}$$

Usually, one can distinguish two different situations when interested about the asymptotics of such models:

(1) The interactions between the agents leads to a state in which all the agents have the same opinion. The opinion value reached is referred to as "consensus" and the network state at this state referred to as "consensus vector".

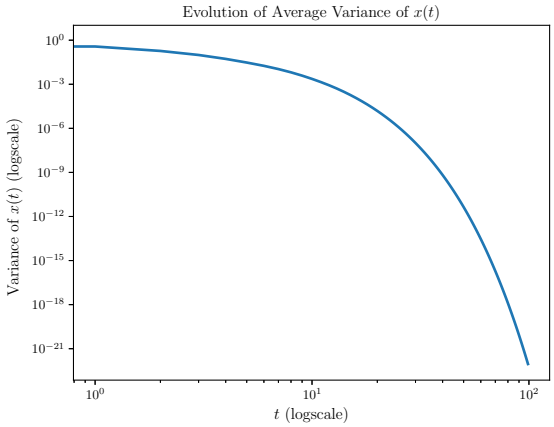

Figure 2: Average Evolution of Variance during time

(2) The interactions between the agents are such that agents do not converge to a shared opinion, i.e. there exists a given pair of agents with different opinions.

Although it may seem counter-intuitive at first, whether or not agents reach a consensus state does not depend on the agents' initial opinions.

That corresponds to the fact that, no matter how polarized are they initially, it is still possible to prove that, under some assumptions, the agents' opinions converge to a shared common value.

In particular, one can prove that, if $\mathcal{G}(\mathcal{V}, \mathcal{E}, W)$ represents a given graph with normalized weight matrix $P = D^{-1}W$ that is aperiodic and has one sink only in its condensation graph, then:

$$\lim_{t\to\infty} P^t x(0) = (\mathbb{1}\pi^\intercal)x(0), \quad \forall x(0) \tag{15}$$

Where π is the unique invariant probability of $\mathcal{G}$ and is computed as the eigenvector associated to the eigenvalue 1 of $P^\intercal$.

This results therefore proves that for aperiodic graphs that have one sink component only the opinion dynamics do converge to a consensus state independently on the initial condition. Nevertheless, the consensus *value* does indeed depend on the initial state, as shown in equation 15.

In light of these theoretical results, and of the fact that $\mathcal{G}(\mathcal{V}, \mathcal{E}, \Lambda)$ is indeed an aperiodic graph with one sink component only in the condensation graph, we simulated N times the opinion dynamics model, each time starting from a different (random) initial condition defined as a discrete uniform in the $[0, 10]$ range and simulating up to $n_{\text{talks}} = 100$ interactions.

Figure 2 shows how the variance of $x(t)$ (averaged over N simulations) evolves as t grows large. In particular, it is possible to see how after a certain value of t the variance in the state vector starts rapidly decreasing, until reaching numerical zero. This clearly shows that the dynamics converged to a consensus state in which all agents have the same opinion.

1.6 Question (f)

Consider an initial condition:

$$x(0) = \vartheta + \{\xi_i\}_{i=1}^{|\mathcal{V}|} \tag{16}$$

Of *i.i.d.* components such that $\mathbb{E}(\xi_i) = \mathbb{E}(\xi) = 0$ and $Var(\xi_i) = Var(\xi) = \sigma^2$

$\overline{Var}(\alpha)$	$Var(\alpha)$	σ^2
2.136e-03	2.068e-03	1e-2
2.136e-02	1.993e-02	1e-1
2.136e-01	2.050e-01	1e0
2.136e+00	2.145e+00	1e1
2.136e+01	2.041e+01	1e2

Table 1: Numerical & Theoretical Results

Then, in light of equation 15, the consensus value $\alpha \in \mathbb{R}$ would be such that:

$$\alpha = \pi^\intercal x(0) \implies Var(\alpha) = Var(\pi^\intercal x(0)) \overset{iid}{=} Var(\xi) \cdot \sum_{i=1}^{\mathcal{V}} \pi_i^2 = \sigma^2 \cdot \sum_{i=1}^{\mathcal{V}} \pi_i^2 \tag{17}$$

Which, since $\pi_i \leq 1 \ \forall i$, clearly implies that $Var(\alpha) \leq \sigma^2$.

We simulated the opinion dynamics process with five different values of σ^2, drawing each time $\tilde{N} = 1000$ initial starting points from a distribution having one of the five different variances. Then, once we simulated the opinion dynamics model, we averaged over all $\tilde{N}$ measurements of variance and obtained an estimate of the consensus variance $\overline{Var}(\alpha)$.

Our numerical results, as well as computations made in light of equation 17, are presented in Table 1.

1.7 Question (g)

Removing edges (d, a) and (d, c) from $\mathcal{G}$ turns the graph presented in Figure 1 into a not fully connected version. Namely, node d becomes a sink, since its out-degree is zero. Moreover, the transition rate matrix becomes:

$$\Lambda_{(g)} = \begin{pmatrix} 0 & 2/5 & 1/5 & 0 & 0 \\ 0 & 0 & 3/4 & 1/4 & 0 \\ 1/2 & 0 & 0 & 1/2 & 0 \\ 0 & 0 & 1/3 & 0 & 2/3 \\ 0 & 0 & 0 & 0 & 0 \end{pmatrix} \tag{18}$$

However, even if the graph is now not connected anymore, its only sink component is still aperiodic, therefore, the opinion dynamics does still converge to a consensus state. Nevertheless, this modification heavily affects the consensus value. However, what changes in this case is the invariant probability $\pi_(g)$.

Even if this new invariant distribution might be computed as the the eigenvector associated to the eigenvalue 1 of $P_{(g)}$, it is possible to obtain it considering the theoretical result that π is always (uniformly, since it always sums up to 1) supported on the nodes of the sink component only. This implies that $\pi_{(g)}$ can be directly derived as:

$$\pi_{(g)} = \begin{pmatrix} 0 & 0 & 0 & 0 & 0 & 1 \end{pmatrix} \tag{19}$$

This implies that the variance of the consensus value, in this case, equals the variance of the starting condition, according to the result presented in equation 17.

We believe this offers an opportunity to briefly reflect on an interesting interpretation of the opinion dynamics model.

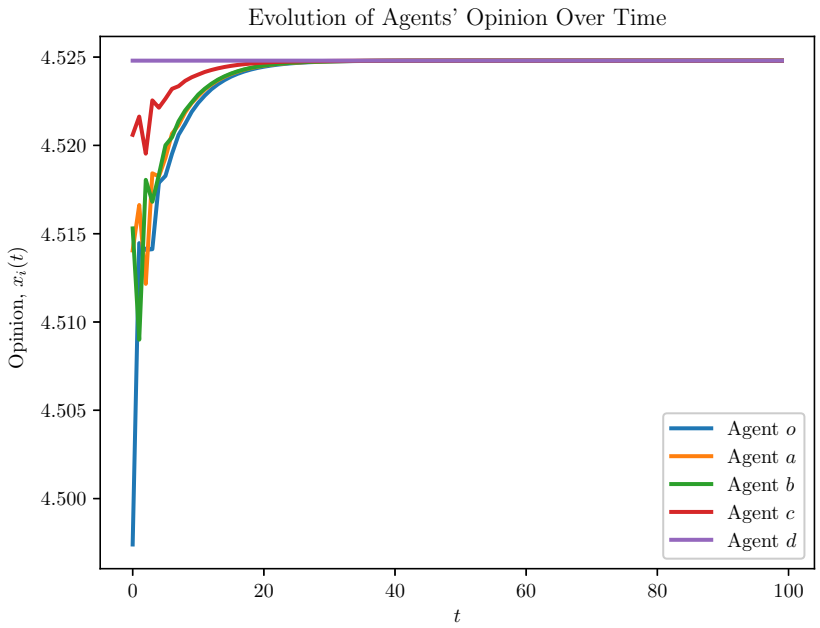

Figure 3: Evolution of Opinions Over Time

As Λ is modified into $\Lambda_{(g)}$, so does P into $P_{(g)}$. However, since P is a row-stochastic matrix, then the whole row related to node d in $P_{(g)}$ is zero but for the diagonal element (which equals 1).

From the model standpoint, this depicts the fact that agent d is updating its own opinion only in light of its own, since it is disconnected from the rest of the network.

However, since other agents update their opinion with respect to d's, the system's opinion long term evolution is going to be completely dictated by agent d opinion.

This also models how stubbornness influences opinion dynamics, to the point in which all the agents end up with the opinion of the stubborn one.

Such a result is presented, averaged over the N different simulations from N randomly chosen starting conditions, in Figure 3.

1.8 Question (h)

Removing edges (c, b) and (d, a) from $\mathcal{G}$ turns the graph presented in Figure 1 into a not fully connected version. Namely, the node set $\mathcal{S} = \{c, d\}$ becomes a sink. The condensation graph of this new modified graph does still present one sink only. However, in this case, the sink component is not aperiodic (as Moreover, the transition rate matrix becomes:

$$\Lambda_{(h)} = \begin{pmatrix} 0 & 2/5 & 1/5 & 0 & 0 \\ 0 & 0 & 3/4 & 1/4 & 0 \\ 1/2 & 0 & 0 & 1/2 & 0 \\ 0 & 0 & 0 & 0 & 2/3 \\ 0 & 0 & 0 & 1/3 & 0 \end{pmatrix} \implies P_{(h)} = \begin{pmatrix} 0 & 2/3 & 1/3 & 0 & 0 \\ 0 & 0 & 0.75 & 0.25 & 0 \\ 0.5 & 0 & 0 & 0.5 & 0 \\ 0 & 0 & 0 & 0 & 1 \\ 0 & 0 & 0 & 1 & 0 \end{pmatrix} \tag{20}$$

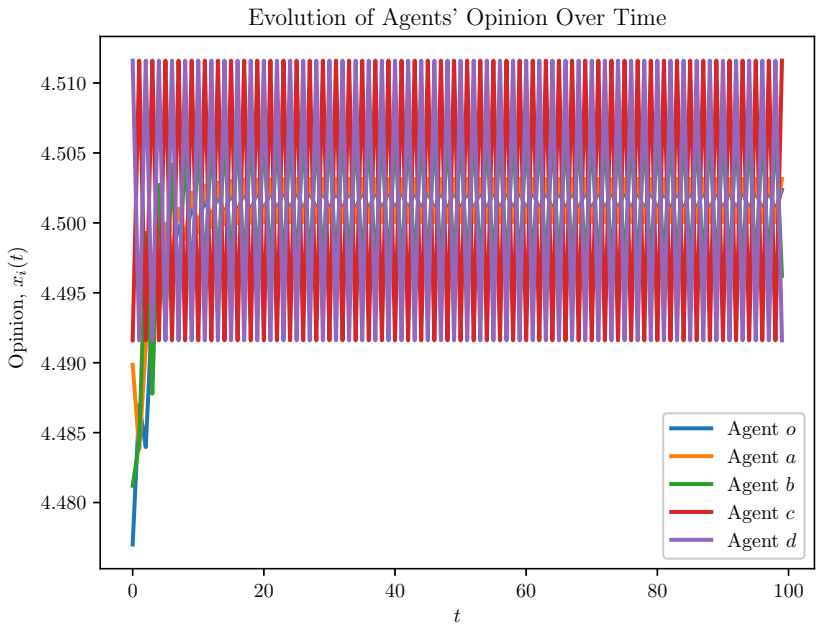

Figure 4: Evolution of Opinions Over Time

Which clearly shows that the minor of $P_{(h)}$ restricted to $\mathcal{S}$ is:

$$P_{(g)}|_{\mathcal{S}} = \begin{pmatrix} 0 & 1 \\ 1 & 0 \end{pmatrix} \tag{21}$$

This matrix still admits a unique leading eigenvector associated to the eigenvalue 1, namely:

$$\pi_{(h)} = \begin{pmatrix} 0 & 0 & 0 & 0 & 1/2 & 1/2 \end{pmatrix} \tag{22}$$

Nevertheless, the dynamics is not guaranteed to converge to a consensus state (in general), since $\mathcal{S}$ is not aperiodic. In this case, the whole evolution of the opinion converges to a consensus state if and only if the initial opinion is a consensus vector of the type:

$$x_i(0) = \begin{cases} 0, & \text{if } i \notin \mathcal{S} \\ \frac{1}{|\mathcal{S}|}, & \text{otherwise} \end{cases} \tag{23}$$

Such a result is presented, averaged over the N different simulations from N randomly chosen starting conditions, in Figure 4, which clearly enough shows the effects that the periodicity of the sink component have on the evolution of the linear averaging dynamics.

Any other starting condition would result in the network not reaching an equilibrium. Therefore, since no variance is admitted in the original opinion (since when it is, the system does not reach any consensus state), we claim that the variance of the consensus value, when defined, is zero.

2 Exercise 2

In this exercise, we still considered the graph presented in Figure 1. Our task was to simulate this system from two different perspectives: the *particle perspective*, i.e. "follow the particle", and the

node perspective, i.e. "observe from the node". Simulating the system from a particle perspective is exactly as in Exercise 1, but here we followed many particles. To simulate the system from the node perspective we observed the particles from the node. When doing this we only cared about the number of particles in the node. Note that at node i, each particle in that node will stay there on average $1/\omega_i$ time units. Therefore, the node will pass along particles at a rate proportional to the number of particles in the node. In fact, if at time t the number of particles in node i is $n_i(t)$, it will pass along particles at a rate of $n_i(t)\omega_i$. The departure times of the node can thus be seen as a Poisson process with rate $n_i(t)\omega_i$. At each tick of the Poisson clock of the node, it will move a particle to a neighboring node. The node to which the particle will move is again based on the normalized transition rate matrix P.

Simulating the system from the two perspectives, we answered the following questions:

Question (a-1) If 100 particles all start in node a, what is the average time for a particle to return to node a?

Question (a-2) How does this compare to the answer in Exercise 1? Why?

Question (b-1) If 100 particles start in node o, and the system is simulated for 60 time units, what is the average number of particles in the different nodes at the end of the simulation?

Question (b-2) Illustrate the simulation above with a plot showing the number of particles in each node during the simulation time.

Question (b-3) Compare the simulation result in the first point above with the stationary distribution of the continuous-time random walk followed by the single particles.

2.1 Question (a-1), (a-2)

To simulate $n_{\text{part.}} = 100$ "random walkers" in the graph presented in Figure 1, we mainly exploited the fact that, in the setting considered (that, for instance, does not consider any constraint on the maximal number of particles that can use a given edge in a certain time window), the $n_{\text{part.}}$ explore the graph *independently*.

Therefore, we basically re-iterated $n_{\text{part.}}$-times the findings of 1.1.

We simulated $j = 1, 2, \ldots, N$ measurements of $(T_a^+)_{p,j}$, of the return time of particle p. We then computed the average return time over all possible simulations *per particle*, i.e.:

$$(\bar{\mathbb{E}}_a(T_a^+))_p = \frac{1}{N}\sum_{j=1}^{N}(T_a^+)_{p,j} \quad \forall p = 1, 2, \ldots, n_{\text{part.}} \tag{24}$$

Lastly, we computed a final estimate of the return time of any particle averaging over all the $n_{\text{part.}}$ estimates of $(\bar{\mathbb{E}}_a(T_a^+))$, i.e.:

$$\bar{\mathbb{E}}_a(T_a^+) = \frac{1}{n_{\text{part.}}}\sum_{p=1}^{n_{\text{part}}}\left(\frac{1}{N}\sum_{j=1}^{N}(T_a^+)_{p,j}\right) = 6.7445 \text{ (t.u.)} \simeq \mathbb{E}_a(T_a^+) \tag{25}$$

This result shows an empirical equivalence with the expected value obtained in 1.1 and it is theoretically justified by the independence of the particles.

2.2 Question (b-1)

To answer this question, we simulated the system from the node perspective considering *local clocks* that have been changing during the simulation. If one indicates with $n(t) \in [0, n_{\text{part.}}]^{|V|}$ the state (number of particles per node) at time t it is clear that each node's rate evolves in time, since it is equal to $n_i(t)\omega_i$.

To obtain this, we designed the following 3-step procedure:

(1) We simulated $|\mathcal{V}|$ realizations of $t^{(i)}_{\text{next}} \quad \forall i = 1, 2, \ldots, |\mathcal{V}|$ and then selected the node that ticked first, that is $v_{\text{quickest}} = \arg\min_{i \in \mathcal{V}}\{t^{(i)}_{\text{next}}\}$. This is the node from which a single particle will move. Note that since by definition $t^{(i)}_{\text{next}} \underset{\omega_i \to 0}{\longrightarrow} +\infty$, it is very unlikely that particles in "empty" nodes move.

(2) Once v_{quickest} would be selected, a particle would then move to a neighbouring node according to the transition probabilities in P. We indicated the node to which the particle would move with v_{next}.

(3) Since the number of particles in two (v_{quickest} and v_{next}) of the $|\mathcal{V}|$ nodes did change, we re-drawn new realizations of $t^{(i)}_{\text{next}} \quad \forall i = 1, 2, \ldots, |\mathcal{V}|$ and went back to (1).

This simulation process would have been repeated until the sum of all the transition instants (that is, the sum of all the *minimal* t_{next}) would be below a given threshold $t_{\max}$.

We simulated this process $\tilde{N} = 500$ times up to $t_{\max} = 60$ time units, always simulating from a configuration in which the number of particles in the system was constant (and, therefore, the particles could only move from node to node according to P). We then computed an estimate of the expected number of particles in each node after 60 time units averaging the final realization of the j-th simulation of the number of particles in each node, that is:

$$\bar{\mathbb{E}}\left(n(t=60)\right) = \frac{1}{\tilde{N}} \sum_{j=1}^{\tilde{N}} n_j(t=60) \simeq \begin{pmatrix} 18 & 18 & 20 & 23 & 21 \end{pmatrix} \tag{26}$$

2.3 Question (b-2)

The average evolution in time of the number of particles in each node of the network is presented in Figure 5.

As a final remark, let us note how the fact that node o quickly loses most of its particles derives directly from the fact that the rate at which node o pass along particles proportionally depends on $n_o(t)$, which is considerably larger than any other $n_i(t)$ up to $t \simeq 5$, since all particles start in o.

2.4 Question (b-3)

To establish a first connection between equation 26 and 7, we mainly leveraged the findings of 2.2. These have been very significant since they showed that in the considered setting each particle moves independently from the others.

This also means that, on average, the probability P_{ij} can be interpreted as the *fraction* of particles that leaves node i to node j, thus allowing to establish a first comparison between the long-term dynamics of random walks and *linear flow dynamics*.

This parallelism mainly plays out in the fact that the (both continuous and discrete time) *linear flow dynamics* evolution is described by equation 5.

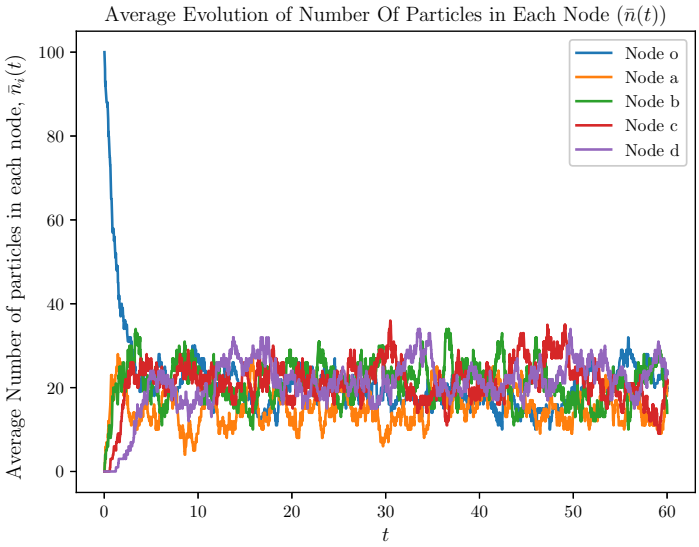

Figure 5: Average Evolution of $n(t)$ over $\tilde{N}$ simulations

Node	**60 t.u.**	**240 t.u.**	$\bar{\pi}$
Node o	18	18	0.1852
Node a	18	16	0.1481
Node b	20	22	0.2222
Node c	23	21	0.2222
Node d	21	23	0.2222

Table 2: Numerical & Theoretical Results when Increasing Simulation Time

Considering this result, we simulated the system $\tilde{N}$ times, each time letting the dynamics pan out for either $t^{(1)}_{\max} = 60$ time units or $t^{(2)}_{\max} = 240$ time units.

In particular, we simulated the dynamic for $t^{(2)}_{\max} = 4t^{(1)}_{\max}$ time units in the sake of analyzing if an increased duration of the simulation would turn out in better approximating the invariant distribution of $\mathcal{G}$.

Our results are presented in Table 2. There we show how increasing the simulation duration (in terms of maximal time the random walk is allowed to evolve) improves the quality of the approximation of the invariant probability, exactly as expected.

For full reproducibility of our experiments, we report that we observed fluctuations in $\bar{n}(t)$ even with 240 time units.

We believe these fluctuations are caused by the fact the overall dynamics do not even approach a stationary distribution in 240 t.u., hence we could improve the numerical stability of our solution by increasing the value of $t_{\text{next}}(2)$.

3 Exercise 3

Consider the open network in Figure 6:

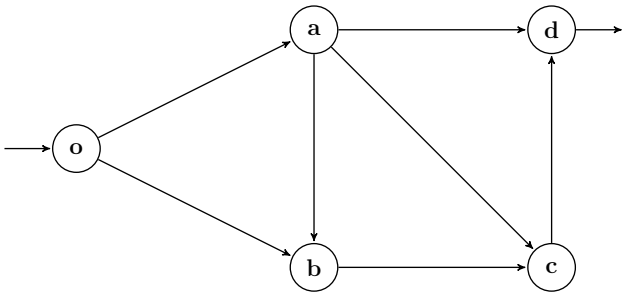

Figure 6: Exercise 3 network

With the following transition rate matrix:

$$\Lambda_{\text{open}} = \begin{pmatrix} 0 & 3/4 & 3/8 & 0 & 0 \\ 0 & 0 & 1/4 & 1/4 & 2/4 \\ 0 & 0 & 0 & 1 & 0 \\ 0 & 0 & 0 & 0 & 1 \\ 0 & 0 & 0 & 0 & 0 \end{pmatrix} \tag{27}$$

We studied how different particles affect each other when randomly moving in continuous time in the network of Figure 6 according to Λ_{open}. For the sake of notation, let us slightly pose $\Lambda_{\text{open}} = \Lambda$.

We analyzed two possible scenarios related to the *rate* at which nodes pass along particles. In particular, we simulated the case in which a given node i would pass along particles at a proportional rate $n_i(t)\omega_i$ or at fixed rate ω_i. We simulated these two different systems to then answer the following questions:

Question (a-1) Simulate the system for 60 time units, in the *proportional rate* case, and plot the evolution of the number of particles in each node over time.

Question (a-2) What is the largest input rate λ that the system can handle before the number of particles in one node eventually diverges?

Question (b-1) Simulate the system for 60 time units, in the *fixed rate* case, and plot the evolution of the number of particles in each node over time.

Question (b-2) What is the largest input rate λ that the system can handle before the number of particles in one node eventually diverges? Why is this different from the other case?

3.1 Question (a-1)

In the process of simulating a system in which nodes pass along particles at proportional rate, we considered the two main stochastic processes characterizing $n(t)$ for the network in Figure 6, from here on-wards referred to as $\mathcal{G}$. Said sub-processes are:

1. The introduction of a new particle from node o, according to a Poisson process with fixed input rate $\lambda = 1$.

2. The movement of particles inside $\mathcal{G}$, similarly to what aforementioned in 2.2. In particular, we modeled the "openness" of $\mathcal{G}$ by either reproducing the results of 2.2 when the source node for the transferal was not d or by reducing the number of particles in d by one, to model fictional particles exiting from $\mathcal{G}$.

We simulated the inherently inter-dependant nature of these two processes similarly to what we did in 2.2. However here we also took care of checking if a particle addition to the system would take place before or after the instant in which a given node *inside the system* ticks and, therefore, a particle moves.

In the case in which new particles are added to the system before than existing ones do move inside it, one simply increments a counter on the number of particles in node o. This also justifies the necessity of recomputing all the $t^{(i)}_{\text{next}} \quad \forall i = 1, 2, \ldots, |\mathcal{V}|$ realizations of the local clocks considered, as $t^{(o)}_{\text{next}}$ clearly depends on $n_o(t)$ in the considered scenario.

However, particles do move *before* an addition takes place, we would merely reproduce the findings of Exercise 2 and recompute every ticking instant but the one of the input particles, which is considered as an input and therefore is not influenced by the evolution of the system (quite the contrary, as it influences it indeed).

For full reproducibility, we report that since $\omega_d = (\Lambda \mathbb{1})_d = 0$, the problem specification requested to impose $\omega_d = 2$. This leads to have that the degree matrix of $\mathcal{G}$ reads:

$$D = \begin{pmatrix} 1.25 & 0 & 0 & 0 & 0 \\ 0 & 1 & 0 & 0 & 0 \\ 0 & 0 & 1 & 0 & 0 \\ 0 & 0 & 0 & 1 & 0 \\ 0 & 0 & 0 & 0 & 2 \end{pmatrix} \tag{28}$$

Whereas, once more, P is simply defined as $P = D^{-1}\Lambda$ and is such that $P_{dd} = 1$.

Our simulation process can be summarized in the following procedure:

(1) Calculate the $t^{(i)}_{next} \quad \forall i \in \mathcal{V}$ and t^{λ}_{next}

(2.a) If $t^{\lambda}_{next} < \min_{\mathcal{V}} t^{(i)}_{next}$, we simulate the introduction of a new particle into the system incrementing the number of particles in node o.

(2.b) Otherwise, we simulate the transition of a particle already existing in the system, exactly as it was done in 2.2. Anyway, we add a new particle in o at t^{λ}_{next}.

We iterated this procedure until the stopping condition of simulating the system for 60 time units was met. We simulated N evolutions of this process and computed various statistics associated to these N realizations of the system.

In Table 3 we present the numerical results of our simulations for what concerns the average final number of particles $\bar{n}(60)$ over N simulations.

Despite witnessing similar results for what concerns the evolution behaviour, here we show one evolution only for practical reasons. This evolution is showed in Figure 7.

In particular, the stopping condition used ($\sum_i t_i \leq t_{\max}$) did yield results with a different number of transitions, preventing us to compute the average evolution without having to resort to some kind of padding).

Moreover, in Figure 8 we show the same process mentioned above, with a particular focus on the number of particles in each single node for visualization readability.

Node	$\lambda = 1$	$\lambda = 1.125$	$\lambda = 1.126$
$\bar{n}_o(t_{\max})$	1.14	1.27	1.24
$\bar{n}_a(t_{\max})$	0.65	0.75	0.74
$\bar{n}_b(t_{\max})$	0.51	0.57	0.57
$\bar{n}_c(t_{\max})$	0.65	0.72	0.74
$\bar{n}_d(t_{\max})$	0.52	0.59	0.58

Table 3: Average Final Number of particles for various values of λ in the proportional-rate scenario.

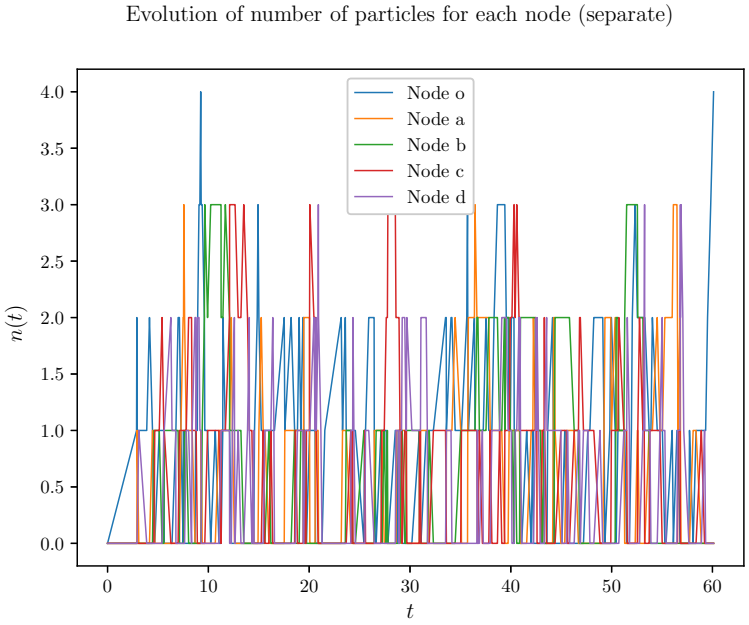

Figure 7: Evolution of number of particles in each node, all together ($\lambda = 1$)

3.2 Question (a-2)

To find the system's breaking point, in principle one could arbitrarily increase the input rate λ until the number of particles in the system diverges. Nevertheless, we believe that this is a fairly brute-force approach that does not exploit the considerable amount of information available for what concerns a more mathematical description of the system dynamics.

The number of particles in each node can indeed be formalized with a set of birth-and-death chains, related to each node in $\mathcal{G}$. In each birth-and-death chain, each node represents the number of particles inside the considered node.

Various theoretical results are available when it comes down to birth-and-death chains. Among them, we believe that one of the most significant is the stationary probability In principle, one should analyze the dynamics associated to every node-specific birth-and-death chain. However, without loss of generality, we formulated the following claim: as node o is the only source node, if the number of particles in node o does blow up, so does the system.

This can be explained considering that, particles from o leave according to P_{oj} $\forall j \in \mathcal{V}$, then it is clear that if $n_o \to \infty$ so does n_j.

On birth-and-death chains of the type considered here (i.e., those in which one can impose balance), one can consider the following equation to obtain the Laplace invariant distribution of

said chain:

$$\bar{\pi}_i = \frac{1}{\zeta} \prod_{j=0}^{i-1} \frac{\lambda_j}{\mu_{j+1}}, \quad i = 0, 1, \ldots, n \tag{29}$$

where $\zeta = \sum_{i \in \{0,1,\ldots,n\}} \bar{\pi}_i$, i represents the number of particles in node o, $\lambda_j = \lambda$ is the system input rate and $\mu_j = j\omega_o$ is the output rate in this case.

The i-th entry of $\bar{\pi}$ represents the probability of being in node i in the birth-and-death chain at stationarity, i.e., the probability that there are i particles in node o.

Considering this result, we reformulated the problem as finding the maximal value of λ so that, given without loss of generality an arbitrarily large maximal capacity for the number of particles in o $c_{\max}$, $\bar{\pi}_{c_{\max}} \to 1$ as $c_{\max} \to \infty$.

To ease up notation, allow us posing $\rho = \frac{\lambda}{\mu}$.

In the *proportional rate* setting considered here one can prove that:

$$\bar{\pi}_{c_{\max}} = \frac{\rho^{c_{\max}}/c_{max}!}{\sum_{j=0}^{c_{\max}} \rho^j/j!} \tag{30}$$

Since the factorial term $c_{\max}!$ clearly dominates the whole fraction, it is easy to see that:

$$\bar{\pi}_{c_{\max}} \to 0 \text{ as } c_{\max} \to \infty \tag{31}$$

As a consequence, the system will never blow up, in keeping with our simulated results.

3.3 Question (b-1)

For what concerns the case in which nodes pass along particles at a fixed rate ω_i, we mainly leveraged the results of previous sections (such as 2.2), although in this case the number of particles is clearly not constant.

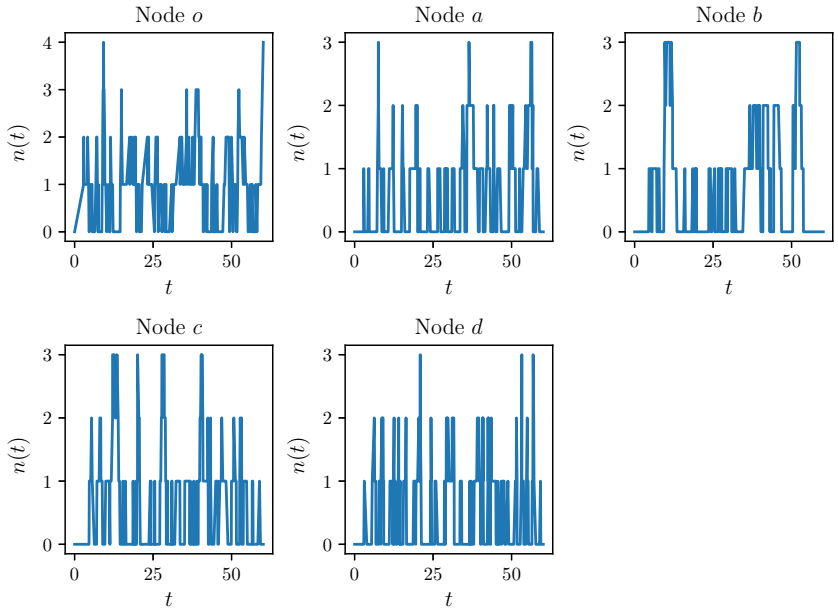

Figure 8: Evolution of number of particles in each node, per node ($\lambda = 1$)

Node	$\lambda = 1$	$\lambda = 1.125$	$\lambda = 1.126$
$\bar{n}_o(t_{\max})$	1.8	6.6	12.1
$\bar{n}_a(t_{\max})$	6.6	1.4	1.2
$\bar{n}_b(t_{\max})$	0.8	1.8	2.1
$\bar{n}_c(t_{\max})$	0.8	1.8	0.8
$\bar{n}_d(t_{\max})$	1.4	1.4	1.4

Table 4: Average Final Number of particles for various values of λ in the fixed-rate scenario.

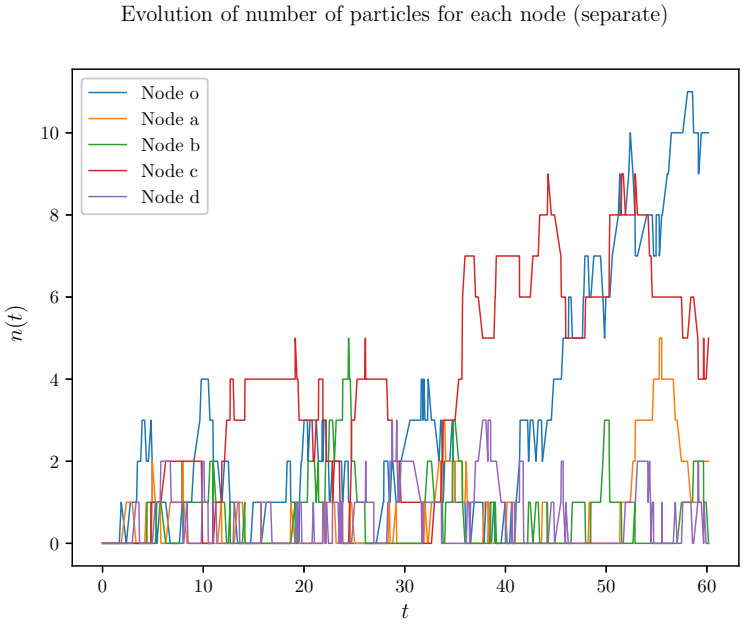

Figure 9: Evolution of number of particles in each node, all together ($\lambda = 1$)

Since the case in which the rate at which nodes pass along particles is fixed can be easily traced back, from a practical standpoint, to the case in which said rate is somewhat proportional, we refer to Question (a-1) for an in-detail explanation of our simulation approach.

In Table 4 we present the numerical results of our simulations for what concerns the average final number of particles $\bar{n}(60)$ over the considered N simulations.

Figure 9 shows the evolution of the number of particles in each node, whereas 10 shows the same process focusing on the evolution of $n_i(t)$ $\forall i \in \mathcal{V}$.

3.4 Question (b-2)

We will follow a similar approach to what we used in Section 3.2, with the sole difference that input and output rates are now both constant. Calling $\rho = \frac{\lambda}{\mu}$, one can prove that the invariant probability distribution reads:

$$\bar{\pi} = \frac{\rho^i}{1 + \rho + \cdots + \rho^n} \implies \bar{\pi}_{c_{\max}} = \frac{\rho^{c_{\max}}}{\sum_{j=0}^{c_{\max}} \rho^j} \tag{32}$$

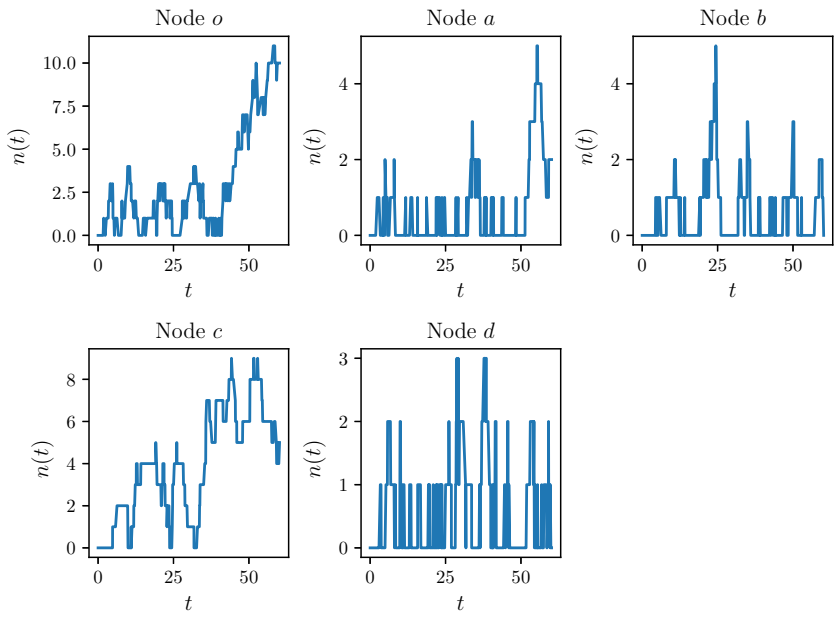

Figure 10: Evolution of number of particles in each node, per node ($\lambda = 1$)

It is easy to see that the the value of $\bar{\pi}_{c_{\max}}$ clearly depends on ρ. In particular, as $c_{\max} \to \infty$,

$$\bar{\pi}_{c_{\max}} = \begin{cases} 1, & \text{if } \rho > 1 \\ 0, & \text{if } \rho \leq 1 \end{cases} \tag{33}$$

This result not only matches our numerical experiments, but also our expectations. Moreover, since $\sum_{j=0}^{c_{\max}}$ diverges as $c_{\max} \to \infty$, equation 33 also captures the probability of an accumulation of resource in a node in which particles exit with a rate larger than the one at which they enter.

As $\mu = \omega_o$, it is enough to set $\lambda > \omega_0 = 1.125$ for $\bar{\pi}_{c_{\max}}$ to approach 1.

Lastly, the largest input rate that the system can handle before blowing up is exactly ω_o, as Table 4 shows.

The whole difference from section 3.2 stems from the different asymptotic behaviour of $\bar{\pi}_{c_{\max}}$.